

Production of Unilamellar Vesicles Using an Inverted Emulsion

Sophie Pautot,[†] Barbara J. Frisken,[‡] and D. A. Weitz^{*,†}

Department of Physics and DEAS, Harvard University, Cambridge, Massachusetts 02138 and
Department of Physics, Simon Fraser University, Burnaby, BC V5A 1S6

Received June 20, 2002. In Final Form: January 2, 2003

We investigate a method for the controlled assembly of unilamellar vesicles consisting of bilayers assembled one leaflet at a time. We use water-in-oil emulsions stabilized by the material for the inner leaflet and produce vesicles by passing the water droplets through a second oil–water interface, where they become coated with the outer leaflet. We have used this technique to form vesicles from lipids, mixed lipid and surfactant systems, and diblock copolymers. The stability of lipid-stabilized emulsions limits the range of sizes that can be produced and the vesicle yield; nevertheless, there are several advantages with this emulsion-based technique: It is possible to make unilamellar vesicles with sizes ranging from 100 nm to 1 μm . Moreover, the process allows for efficient encapsulation and ensures that the contents of the vesicles remain isolated from the continuous aqueous phase. To illustrate possible applications of this technique, we demonstrate the use of vesicles as microreactors where we polymerize actin through the addition of magnesium and show that the polymerization kinetics are unaffected by the encapsulation.

Introduction

Bilayers of lipid molecules that fully enclose a fixed volume of fluid are called vesicles or liposomes. They are ubiquitous in cells where they encapsulate and isolate intracellular fluids and often contain specific proteins or other macromolecules. Vesicles are also used to transport macromolecules through the blood stream or through the skin, leading to the widespread use of vesicles in cosmetics and drug delivery.^{1–3} In addition, they serve as a model system for the study of the fundamental properties of lipid bilayer membranes. Ideally, these applications require simultaneous control of vesicle size, unilamellarity, encapsulation yield, biocompatibility, and lipid composition, but none of the vesicle production techniques currently used fulfills every requirement. Sonication can be used to produce vesicles with radii smaller than 50 nm (small unilamellar vesicles or SUV) but this produces a highly heterogeneous size distribution.^{4–6} Alternatively, large multilamellar vesicles (MLV), formed spontaneously in excess water, can be extruded through a narrow pore size filter to produce a more monodisperse distribution of large unilamellar vesicles (LUV).⁷ By contrast, production of giant unilamellar vesicles (GUV) that range in size from 1 to 20 μm is usually accomplished by rehydration or swelling⁸ thin lipid films with water or by electroformation,⁹ the resultant suspension contains a broad distribution of sizes, and only a few of the vesicles produced are

unilamellar. Vesicles produced by all of these techniques are formed in the same medium that they encapsulate, which limits their utility for encapsulation of precious drugs or other active agents available in limited quantities. One technique, called reverse evaporation,¹⁰ overcomes this deficiency but depends on the use of organic solvents, trace amounts of which remain in the bilayer and can contaminate the internal aqueous phase. Finally, to successfully produce vesicles, each technique has specific requirements for either the lipids or the buffer used. This lack of flexibility has negatively impacted the use of vesicles for drug delivery; their role is typically limited to that of simple carrier rather than the dynamic and functional compartments they could become.

To help overcome some of these limitations, we have investigated a method of vesicle production that involves the assembly of two independently formed monolayers of amphiphilic molecules into unilamellar vesicles. The first step is the preparation of a stable inverted emulsion, as shown in Figure 1A. The aqueous solution to be emulsified is mixed with the oil phase containing surfactant molecules. As the water drops are formed, the surfactant molecules dispersed in the oil adsorb at the surface of the drops to form a monolayer that helps stabilize the emulsion, reducing coalescence of the drops. This monolayer will form the inner leaflet of the bilayer that will make up the final vesicle bilayer. We then pour a second oil phase, also containing surfactant molecules, over the top of an aqueous phase, as shown in Figure 1B. Because the oil is less dense, it remains above the aqueous phase, and surfactant molecules dispersed in the oil phase diffuse from the bulk to the water/oil interface to form a monolayer. After the interface is fully covered, we gently pour the inverted emulsion on top of the oil–buffer interface as shown in Figure 1C. The water droplets in the inverted emulsion are heavier than the oil phase and sediment toward the oil–buffer interface. Upon crossing the interface, the emulsion droplets pick up a second layer of lipid, forming a bilayer and transforming the emulsion

[†] Harvard University.

[‡] Simon Fraser University.

(1) Gregoriadis, G. *FEBS Lett.* **1971**, *14*, 95.

(2) Nicolau, C.; Paraf, A. *Liposomes, drugs and Immunocompetent Cell Functions*; Academic Press: New York, 1981.

(3) Barron, L. G.; Meyer, K. B.; Szoka, F. C. *J. Hum. Gene Therapy* **1998**, *9*, 315–323.

(4) Gregoriadis, G. *Preparation of Liposomes*; CRC Press: Boca Raton, FL, 1984; Vol. 1.

(5) Ostro, M. J. *Liposomes*; Marcel Dekker Inc.: New York, 1983.

(6) Philippot, J. R.; Schubert, F. *Liposomes as Tools in Basic Research and Industry*; CRC Press: Boca Raton, FL, 1995.

(7) Olson, F.; Hunt, C. A.; Szoka, F. C.; Vail, W. J.; Papahadjopoulos, D. *Biochim. Biophys. Acta* **1979**, *9*, 557.

(8) Lasic, D. D.; Yechezkel, B. *Handbook of Non Medical Applications of Liposomes*; CRC Press: Boca Raton, FL, 1996.

(9) Angelova, M. I.; Dimitrov, D. S. *Faraday Discuss.* **1986**, *81*, 303.

(10) Szoka, F.; Papahadjopoulos, D. *Proc. Natl. Acad. Sci.* **1978**, *75*, 4194–4198.

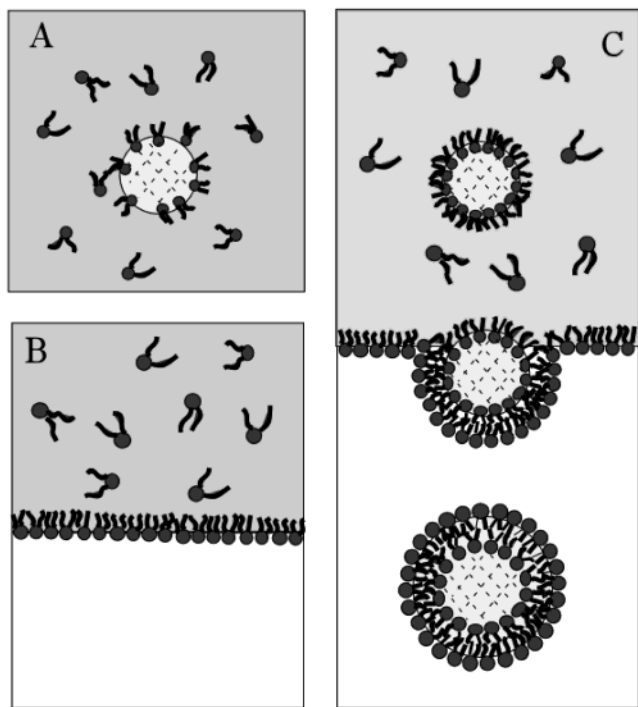


Figure 1. Schematic illustration of the synthesis of vesicles from an inverted emulsion. (A) Water is emulsified in oil with lipid as the surfactant, forming a stable inverted emulsion. (B) The water that will receive the final vesicles is placed in a second vial, and lipid-saturated oil is poured on top of it. A lipid monolayer forms at the oil–water interface. (C) Preparation A is then gently poured on top of preparation B. The inverted emulsion droplets are heavier than the oil that contains them and sediment into the second water phase. As they pass through the interface where the second layer of lipid is sitting, the bilayer is completed and the final vesicles are formed.

droplets into unilamellar vesicles. After sedimentation, the vesicles are in the bottom aqueous buffer.

An emulsion-based method of vesicle production has several obvious advantages. During the entire process, the encapsulated material remains distinct from the hosting buffer. The vesicles are thus filled with the solute of interest directly during their formation, making high encapsulation efficiency possible. The use of emulsification for encapsulation in the first step makes it independent of the type of amphiphilic molecule used, of the size or charge of the macromolecules to be encapsulated, or of the ionic strength of the buffer. It improves the fabrication of unilamellar vesicles by making a wider range of sizes accessible with a single technique. It provides a means to control the composition of each leaflet making it possible to use a broader choice of amphiphilic molecules to assemble the bilayer. It also makes it possible to form asymmetric bilayers. Because every component of the vesicle can be controlled, this technique provides the potential for new applications in biomaterials engineering including the possibility of transforming these vesicles into microreactors where reactive molecules can be efficiently encapsulated and isolated from the bulk and where remotely triggered reactions can occur.

This method has been discussed before but has not been implemented widely. It was demonstrated as a method of vesicle production using a benzene:water:egg-PC emulsion, and the possibility of making asymmetric vesicles was proposed.¹¹ More recently, an encapsulation efficiency

of 60% was reported using vesicles produced from a decane:water:egg-PC emulsion.¹² In both cases, sonication was used to prepare the initial emulsion and electron microscopy was used to determine the vesicle sizes; they were consistently less than 200 nm in diameter.

In this paper, we present a detailed description of the inverted-emulsion method and we discuss its limitations. We show that, by application of suitable emulsification techniques, it is possible to make vesicles ranging in size from 0.1 μm to 1 μm with a variety of surfactant-like molecules. We demonstrate that the vesicles are unilamellar and that it is possible to achieve encapsulation efficiencies as high as 98%. In other work,¹³ we show that it is possible to use this technique to make asymmetric vesicles. We also discuss limitations to this technique that occur when lipids are used to stabilize the emulsion; these include control of the size and number of vesicles formed. We have observed that lipids do not behave like most surfactants. Thus, the emulsification process is sometimes not fully controlled and the slow equilibration of lipid monolayers at oil–water interfaces limits replenishment of this interface and thus vesicle yield. We discuss the behavior of lipids in an oil–water environment and how this impacts the control of the size of the emulsion, the composition of each leaflet of the bilayer, and ultimately the number of vesicles produced. Finally, to illustrate the potential of this technique, we demonstrate the encapsulation of a variety of molecules without loss of their activity and show that it is possible to use vesicles as microreactors.

Materials and Methods

Materials. The lipids used included egg-PC (egg-phosphatidylcholine), POPC (1-palmitoyl-2-oleoyl-sn-glycero-3-phosphocholine), POPS (1-palmitoyl-2-oleoyl-sn-glycero-3-phospho-L-serine), and DOPS (dioleoyl-sn-glycero-3-phospho-L-serine). We also used fluorescently labeled lipids including NBD-PC (1-palmitoyl-2-(6-((7-nitro-2-1,3-benzoxadiazol-4-yl) amino) caproyl)-sn-glycero-3-phosphocholine) and NBD-PS (1-palmitoyl-2-(6-((7-nitro-2-1,3-benzoxadiazol-4-yl) amino) caproyl)-sn-glycero-3-(phospho-L-serine)) and rhodamine-DHPE (1,2-dihexadecanoyl-sn-glycero-3-phosphoethanolamine). All of these lipids were purchased from Avanti Polar Lipids, Inc. (Alabaster, AL) as 99% pure chloroform stock solution and were used without further purification. Biotin-conjugated lipid (N-((6-biotinoyl)amino)hexanoyl)-1,2-dihexadecanoyl-sn-glycero-3-phosphoethanolamine was obtained from Molecular Probes (Eugene, OR). A diblock copolymer PABu-PAM provided by Rhodia (Cranbury, NJ) was used to prepare polymersomes. This is a symmetric diblock copolymer composed of a polybutylacrylate block and a polyacrylamide block, both with $M_w = 8000$ g/mol.

The encapsulation of macromolecules was demonstrated with a 1 wt % solution of dextran, $M_w = 10\,000$ g/mol, tagged with Texas Red (Molecular Probes, Eugene, OR). The encapsulated solution used to probe the transport of divalent cations across the bilayer was a polymer solution prepared by suspending 10 000 M_w dextran tagged with Oregon Green 488 bapta-1, a calcium sensitive dye (Molecular Probes, Eugene, OR), in an aqueous buffer consisting of 0.1 M KCl with 10 mM Tris at pH = 8. The solution was dialyzed overnight against a buffer free of calcium and magnesium to remove divalent cations that might be present in the polymer powder; the final concentration was then set at 1 mg/mL. Finally, to study the polymerization of actin inside the vesicles, we used actin from *Acanthamoeba* purified according to the protocol established by Gordon et al.¹⁴ We prepared N-(1-pyrenyl) iodoacetamide-labeled F-actin¹⁵ and used 20% labeled

(12) Zhang, L.; Hu, J.; Lu, Z. *J. Colloid Interface Sci.* **1997**, *190*, 76–80.

(13) Pautot, S.; Frisken, B. J.; Weitz, D. A. Unpublished.

(14) Gordon, D. J.; Eisenberg, E.; Korn, E. D. *J. Biol. Chem.* **1976**, *251*, 4778–4786.

(15) Kouyama, T.; Mihashi, K. *Euro. J. Biochem.* **1981**, *114*, 33–38.

(11) Trauble, H.; Grell, E. *Neurosci. Res. Programm Bull.* **1971**, *9*, 373–380.

actin and 80% nonlabeled actin to study the kinetics of polymerization of the actin upon addition of magnesium.

Preparation of the Vesicles. The choice of the organic phase used to prepare the inverted emulsion is dictated by the balance between the solubility of the lipid in oil, the stability of the inverted emulsion, and the possible presence of oil in the final bilayer. Unlike previous attempts to use similar techniques,^{12,16,17} we use a sufficiently long-chain alkane to ensure that the alkane molecules are not incorporated into the final bilayer¹⁸ and that a stable, inverted macroemulsion is formed. We observed that the use of alkanes with chains shorter than 10 carbons resulted in a microemulsion where we were no longer able to control the size of the water droplets. We found that dodecane, a 12 carbon alkane, was most suitable for our applications, but a variety of oils can be used. Alkanes with chain lengths ranging from 12 to 17 carbons resulted in stable macroemulsions, as was squallene, a complex carbon alkane chain of high molecular weight. We have checked the composition of the bilayer by making a thin-layer chromatography analysis of the final vesicles and comparing this to that of pure lipids and pure alkane samples. We could not detect the presence of alkane indicating that, if alkane molecules were present, they made up less than 5% of the bilayer. This is the sensitivity limit of this technique; other techniques were not pursued. The best alkane for an oil-free bilayer is squallene, which has the advantage that it is immiscible in lipid bilayers¹⁸ while still providing a good continuous phase for emulsion preparation.

A wide variety of surfactants can be used to stabilize an inverted emulsion. In this work, we used nonionic surfactants, lipids, and diblock copolymers, chosen according to geometrical arguments¹⁹ such that

$$\left(\frac{v}{a_0 l_c}\right) \geq 1 \quad (1)$$

where v is the volume of the hydrocarbon chain, a_0 is the surface area of the polar head, and l_c is the chain length. When this ratio is greater than one, the area of the hydrophobic part of the molecule is larger than that of the hydrophilic part, which favors the stabilization of an inverted emulsion. Lipids have a ratio only slightly higher or lower than one depending on the polar headgroup and salt conditions; this fact makes them a poor surfactant with which to stabilize an emulsion.

The inverted emulsion was usually prepared by first dispersing the surfactant in the oil phase. For multicomponent lipid mixtures, the lipids were first dissolved together in chloroform to obtain a homogeneous dispersion. The chloroform was then evaporated under a stream of nitrogen to form a dry thin film on the surface of a glass vial, which swelled easily when dodecane was added. To fully disperse the lipid molecules in dodecane, the suspension was placed in a sonication bath overnight at 25 °C. Surfactants in liquid form, like Span80, a nonionic surfactant, were added directly to the dodecane. Finally, for samples prepared with the diblock copolymer PABuPAM (Rhodia, Cranbury, NJ), it was more convenient to dissolve the powder directly in the aqueous solution at 0.1 wt % to prepare the inverted emulsion.

The emulsification of the aqueous solution and surfactant-saturated dodecane can be achieved by various methods.²⁰ The amount of shear and the method by which it is applied to the suspension are responsible for the mean size and polydispersity of the emulsion produced. Four different emulsification techniques were used: shear by gentle stirring, shear using a mixer, extrusion, and sonication. For lipids and nonionic surfactants, a crude inverted emulsion was prepared either by vortexing the solution for several minutes or by gently stirring the suspension with a magnetic stir bar for 1–3 h. The emulsion produced was

very polydisperse with a mean size around 1 μm . More controlled preparation was achieved by using a shear mixer with variable rotation speed (Ultra-Turrax T25, IKA, Wilmington, NC) or extrusion of the suspension through a narrow pore size polycarbonate filter (Poretics Corp., Livermore, CA). Extrusion was also used to reduce the polydispersity and the size of the droplets in an emulsion produced by other techniques. Further purification steps are then required to extract the inverted emulsion.²¹ Finally, in some cases, such as the diblock copolymer, the best results were obtained by sonicating the suspension. Unless otherwise specified, the emulsified aqueous solution consisted of 100 mM NaCl and 5 mM Tris buffered at pH = 7.4. The volume fraction of the aqueous solution was 0.5% of the total volume.

To prepare for the final step in the assembly, we placed 3 mL of aqueous buffer in a centrifuge tube (Falcon tube, 50 mL with a 1-in. diameter) and then gently poured about 2 mL of dodecane containing amphiphilic molecules for the outer monolayer on top of the buffer. Some of these molecules diffused to cover the oil–water interface. For most surfactants, adsorption at an interface is diffusion limited²² and full coverage should occur in only a few minutes. The adsorption mechanism for lipids appears to be more complex; we found that it takes from 30 min for charged lipids up to 90 min for zwitterionic ones to achieve full coverage.²³ Once the interface was fully covered, the inverted emulsion was added to the Falcon tube. The volume of the emulsion added was varied from 0.1 mL to 1 mL to ensure that the total area of the emulsion did not exceed the total area of the monolayer available to supply the outer leaflet. After the three layers were assembled, the tube was placed in a spin-bucket centrifuge and spun at 120 g for 5–10 min. Since water is denser than oil, the water droplets sediment toward the oil–buffer interface. Centrifugation was used to enhance the rate of sedimentation, decreasing the time required to transfer the droplets from several hours to a few minutes.

Characterization. (1) *Microscopy.* All of our real-space observations were done using an inverted microscope (Leica) used either in normal or confocal mode. Some of the pictures were obtained with a 100x phase contrast oil immersion objective while the fluorescence pictures were obtained with a 100x DIC oil immersion objective.

Since freely diffusing vesicles smaller than 1 μm move in and out of the focus plane rapidly, it is difficult to image them and measure their size by microscopy. To overcome this, we used streptavidin/biotin chemistry²⁴ to fix the vesicles to the coverslip, confining them to a plane and improving the image. For this purpose, vesicles were prepared with 1% biotin-conjugated lipid. After the vesicles were made, they were first incubated with a 1:1 molar ratio of free streptavidin (Sigma, St. Louis, MO) for 15 min, resulting in streptavidin-coated vesicles, and were then incubated for 10 min on a cover glass previously coated with biotinylated albumin (Sigma, St. Louis, MO). The cover glass was washed five times with buffer to eliminate unbound vesicles. The bound vesicles did not seem to adhere to the coated cover glass with a wide contact area; although attached to the surface, they still moved about their anchoring point, suggesting that the binding was relatively weak.

(2) *Fluorescence Experiments.* Fluorescence measurements were performed on a luminescence spectrometer (Perkin-Elmer LS 50B). The instrument was used to monitor changes in the intensity of emitted light of wavelength λ_{em} for a fixed excitation wavelength λ_{exc} while the local environment of the dye was modified. Experimental parameters such as excitation and emission wavelength were determined by measuring the excitation and the emission spectrum for each sample.

We used a fluorescence quenching assay^{25,26} to measure the distribution of tagged lipids between inner and outer monolayers.

(16) Szoka, F. C.; Papahadjopoulos, D. *Annu. Rev. Biophys. Bioeng.* **1978**, *9*, 467–508.

(17) Xiao, Z. D.; Huang, N. P.; Xu, M. H.; Lu, Z.; Wei, Y. *Chem. Lett.* **1998**, *3*, 225.

(18) McIntosh, T. J.; Simon, S. A.; MacDonald, R. C. *Biochim. Biophys. Acta* **1980**, *597*, 445–463.

(19) Israelachvili, J. *Intermolecular and Surface Forces*; Academic Press: London, 1992.

(20) Hunter, R. J. *Foundations of Colloid Science, Volume II*; Oxford Science Publications: New York, 1989.

(21) Bibette, J. J. *Colloid Interface Sci.* **1991**, *147*, 474–478.

(22) Ferri, J. K.; Stebe, K. J. *Adv. Colloid Interface Sci.* **2000**, *85*, 61–97.

(23) Pautot, S.; Frisken, B. J.; Cheng, J.-X.; Xie, S.; Weitz, D. A. Unpublished.

(24) Bayer, E. A.; Wilchek, M. *Methods Biochem. Anal.* **1980**, *26*, 1–45.

(25) McIntyre, J. C.; Sleight, R. G. *Biochemistry* **1991**, *30*, 11819–11827.

(26) Gruber H. J.; Schindler, S. H. *Biochim. Biophys. Acta* **1994**, *1189*, 212–224.

A suspension of vesicles was prepared with 0.5% of a fluorescently labeled lipid. The fluorescence of the vesicle solution was measured before and after addition of a quenching solution of sodium hydrosulfite (1 M Na₂S₂O₄ in 5 mM TES at pH = 9, prepared daily). When in the vicinity of the fluorophore, the sodium hydrosulfite extinguishes the fluorescence by reducing the dye. As this molecule does not diffuse across the lipid bilayer, the addition of the quencher to the vesicle suspension results in the extinction of only the dye located on the outer leaflet of the bilayer. The dye on the inner leaflet was exposed by adding detergent (Triton X-100 reduced) to lyse the bilayer. The excitation wavelength for these measurements was set at $\lambda_{\text{exc}} = 470$ nm, and the emission of fluorescence was measured at $\lambda_{\text{em}} = 550$ nm.

Finally, fluorescence measurements were used to probe the polymerization of pyrene-labeled actin protomers. Polymerization of actin containing 20% actin protomer labeled with pyrene leads to an increase in fluorescence intensity of the pyrene.¹⁵ This increase in fluorescence is due to a modification of the pyrene environment when the actin protomers associate during the polymerization. Furthermore, the spectral signature of pyrene F-actin is slightly different from pyrene G-actin allowing the polymerization to be monitored. The excitation wavelength used was $\lambda_{\text{exc}} = 365$ nm, and the change in the emitted fluorescence intensity was monitored at $\lambda_{\text{em}} = 407$ nm after the polymerization was initiated by the addition of salt.

(3) *Dynamic Light Scattering.* The apparatus used for the light-scattering experiments was an ALV DLS/SLS-5000 spectrometer/goniometer (ALV-Laser GmbH, Langen, Germany). The light source for the experiments was an argon ion laser of wavelength 514.5 nm (Coherent, CA). Light scattered by the sample was detected at an angle of 90° from the transmitted beam, where the effects of reflection are minimized. The sample cell was placed in a toluene bath maintained at a temperature of 25 °C.

The size and size distribution of the inverted emulsion and the vesicles were characterized by dynamic light-scattering (DLS) measurements. In DLS, we measure the normalized time autocorrelation of the intensity of the scattered light $g^{(2)}(\tau)$, which is related to the time autocorrelation function of the scattered electric field light $g^{(1)}(\tau)$.²⁷ For a dilute suspension of monodisperse particles, $g^{(1)}(\tau)$ decays exponentially with a decay rate $\Gamma = Dq^2$, where q is the magnitude of the scattering wave vector and D is the diffusion coefficient, which can be related to the hydrodynamic radius through the Stokes–Einstein relation. For a polydisperse sample, $g^{(1)}(\tau)$ is no longer a single exponential because particles with different sizes have different diffusion coefficients and hence different decay rates. The effect of a distribution of decay rates $G(\Gamma)$ on $g^{(1)}(\tau)$ is given by

$$g^{(1)}(\tau) = \int_0^\infty G(\Gamma) e^{-\Gamma\tau} d\Gamma \quad (2)$$

A regularized fit routine supplied by the ALV instrument, which is similar to CONTIN 2DP,^{28,29} was used to obtain $G(\Gamma)$ when an expansion in term of cumulants³⁰ failed to fit the data because the size distribution was multimodal. The resulting distributions have to be viewed with considerable caution, and they are used here only to estimate the populations present in our samples when other types of analysis are not possible.

Vesicle Production

Characterization. (1) *Visualization.* The vesicles produced with this technique can be visualized by microscopy. Figure 2A shows an image, obtained with phase contrast microscopy, of polydisperse vesicles prepared from an inverted emulsion. The emulsion was prepared by gently stirring for 3 h 1 vol % aqueous buffer in dodecane containing 0.05 mg/mL POPC. The resulting emulsion was polydisperse with droplet sizes ranging from

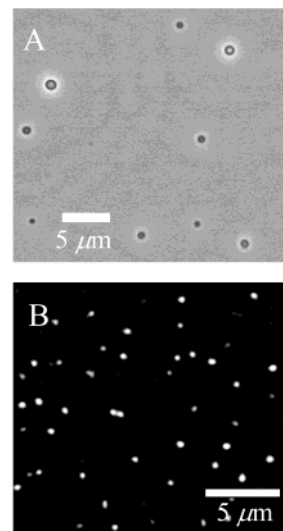


Figure 2. (A) Phase contrast microscopy image of larger, polydisperse POPC vesicles assembled using an inverted emulsion prepared with a low-shear technique. (B) Fluorescence microscopy images of egg-PC vesicles formed from an emulsion extruded through a 1- μm filter.

1 to 4 μm in diameter. Figure 2B shows a suspension of monodisperse egg-PC vesicles obtained from an emulsion that was extruded several times through a 1- μm pore filter. One mole % of rhodamine was mixed with the egg-PC to allow visualization by fluorescence microscopy, and 1 mol % of biotin-conjugated lipid was added so that the vesicles could be bound to a streptavidin substrate. The emulsion used in this preparation was composed of drops about 500 nm in diameter, as well as some much larger drops of aqueous phase that was not fully emulsified, which were not used in the vesicle preparation.

The vesicles that could be made most easily were relatively small in size, less than ~ 500 nm in diameter; we found that the size distribution of these smaller vesicles was determined by that of the initial inverted emulsion. To illustrate this, we compare the autocorrelation functions measured for a vesicle sample with that of the inverted emulsion used to prepare it in Figure 3A. The inverted emulsion, stabilized with POPC and prepared by gentle stirring, was used to form vesicles after the larger drops had been removed by sedimentation. After the time scale for the emulsion data has been scaled by the ratio of the viscosities, the autocorrelation function for the inverted emulsion (triangles) is virtually indistinguishable from that of the vesicles (circles). The distributions of decay times are shown in Figure 3B. The distribution for the inverted emulsion is slightly broader, perhaps because of the presence of lipid aggregates in the sample. The mean of the two distributions is comparable; the mean radius of the emulsion distribution is 220 nm where that of the vesicle distribution is 170 nm. These results confirm that the size of the inverted emulsion dictates the size of the vesicles for these small droplets.

(2) *Determination of Vesicle Unilamellarity.* We used a fluorescence quenching assay to determine the lamellarity of the vesicles. Figure 4 shows the time-dependence of the fluorescence intensity of POPS:NBD-PS vesicles made from an emulsion prepared by gentle stirring. At the first arrow, 60 μL of quencher solution was added. As the quencher diffuses to the surface of the vesicles, the intensity decreases and finally reaches a plateau when the fluorescence of all the NBD-PS lipids present in the outer leaflet of the bilayer has been extinguished. At the second arrow, Triton-X-100 was added. As the vesicles

(27) Berne, B. J.; Pecora, R. *Dynamic Light Scattering*; John Wiley and Sons: New York, 1976.

(28) Provencher, S. W. *Comput. Phys. Commun.* **1982**, *27*, 213–227.

(29) Provencher, S. W. *Comput. Phys. Commun.* **1982**, *27*, 229–242.

(30) Koppel, D. E. *J. Phys. Chem.* **1972**, *52*, 4814–4820.

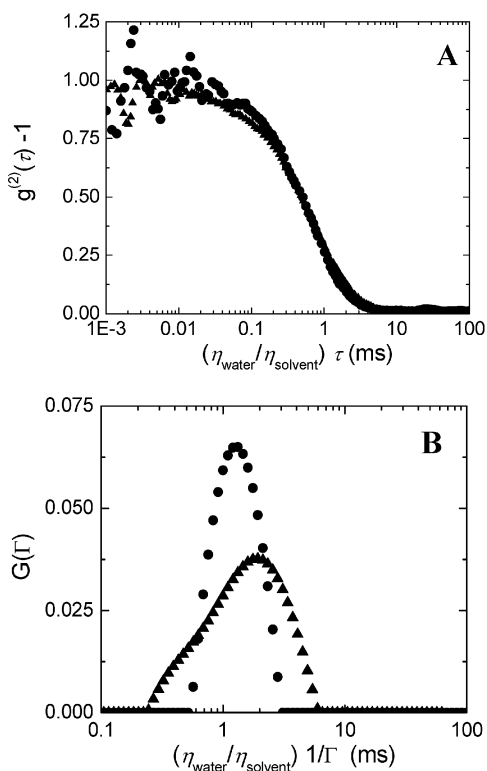


Figure 3. Comparison of the distribution of sizes between the emulsion and vesicles when the inverted emulsion contains small ($<1\mu\text{m}$) droplets. (A) The autocorrelation function $[g^{(2)}(\tau) - 1]$ obtained by DLS at a scattering angle of 90° for a stable inverted emulsion stabilized by POPC (triangles) and from the vesicles produced from it (circles). The data have been corrected for the difference in viscosity. We plot in (B) the distribution of decay times obtained using ALV's regularized fit routine for the emulsion (triangles) and for the vesicles produced from it (circles), again corrected for the difference in viscosity. The distribution for the emulsion is broader than that for the vesicles but their mean values are essentially the same.

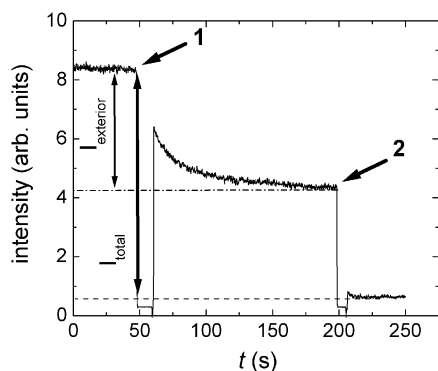


Figure 4. Fluorescence measurements of intact POPS:NBD-PS vesicles begins at time $t = 0$. Addition of sodium hydrosulfite occurred at arrow 1. The fluorescence of the vesicles decreased to a plateau value, which represents the fluorescence intensity due to the inner leaflet only. At arrow 2, Triton-X-100 reduced was added to lyse the vesicles. The fluorescence decreased to background levels as the inner lipids were exposed to the quencher. In this experiment, 48% of the fluorescent lipid is located in the outer leaflet, implying that the vesicles formed with our technique are unilamellar.

break up and the NBD-PS lipids present on the inner leaflet are exposed to the quencher, the intensity reaches its minimum value. To calculate the lamellarity, we assume that the first intensity drop is proportional to the concentration of NBD-PS on the outer leaflet of the bilayer

and that the difference between initial and final values is proportional to the total concentration of NBD-PS present in the sample. We calculate the ratio of these measurements to be 0.48, consistent with an equal distribution of dye on the outer and inner layer and vesicles that are unilamellar.

Limitations of the Technique. This technique relies on the formation of a stable inverted emulsion and on the passage of the emulsion droplets through a second interface to make the bilayer. Unfortunately, both of these steps create problems when lipids are used and limit the generality and practicality of this technique. The problems originate from the use of lipids in the role of surfactants. First, lipids form large aggregate structures in both oil and water and hence do not stabilize the interface of the emulsion as well as a traditional surfactant can; this severely limits the effectiveness of the emulsification and restricts the concentration of water that can be emulsified. Second, lipids adsorb very slowly to the interface and require extended periods of time to fully cover the surface; as a result, the emulsion drops are much less robust and require an equilibration time of at least 30 min. Third, lipids at the interface between oil and water apparently undergo spontaneous emulsification; this seems to result in a strongly preferred drop size, making it exceedingly difficult to produce drops of arbitrarily controlled sizes. Fourth, the slow equilibration of the interface makes it difficult to replenish the second interface as the emulsion drops pass through it; this severely limits the efficiency of the formation of the vesicles, particularly as the size of the droplets increases. The combination of these effects severely limits the usefulness of the technique. We emphasize, however, that despite these limitations, this method does allow the efficient production of uniformly sized, unilamellar vesicles with a far greater range of sizes than is attainable with other techniques and in a manner that allows efficient encapsulation. However, to help establish the range of validity of this method, we elaborate on these limitations:

(1) *Stability of the Emulsion.* We observe that the lipid will partition between the dodecane and the aqueous phase for volume fractions of water greater than 1%; an example is shown in Figure 5. This sample consists of an inverted emulsion prepared by sonication and containing dodecane, 0.5 mg/mL POPC, and 1 vol % aqueous buffer. The final suspension contains both inverted emulsion drops, shown in Figure 5A, and larger emulsion drops containing vesicles, shown in Figure 5B. The large emulsion drops shown in Figure 5B eventually coalesce with one another and phase separate. This tendency of the emulsion to destabilize at high water contents was observed in a wide variety of lipids and for emulsions made by different techniques. It was more likely to occur at higher temperatures. We believe that this behavior occurs because the geometrical shape of the lipid is marginally suitable for emulsion formation, since the hydrophilic and the hydrophobic areas have comparable size. To prevent phase separation of the emulsion at room temperature, our emulsions contained no more than 1 vol % aqueous solution and 0.05 mg/mL lipid. In some cases, these quantities can be increased by the addition of small fraction of a suitable surfactant, such as Span-80. This partitioning sets a stringent limit on the number of vesicles that can be produced and requires a very delicate balance of concentrations to attain suitable conditions to produce a stable inverted emulsion.

(2) *Equilibration of the Emulsion.* This technique relies on the formation of stable oil-water interfaces fully covered with lipids. However, the formation of a fully

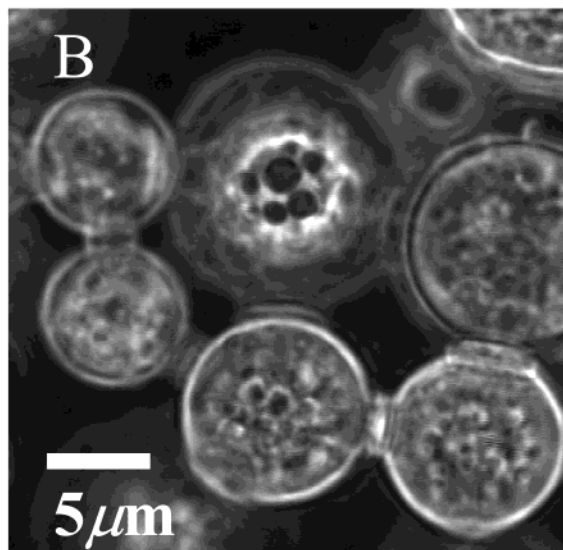
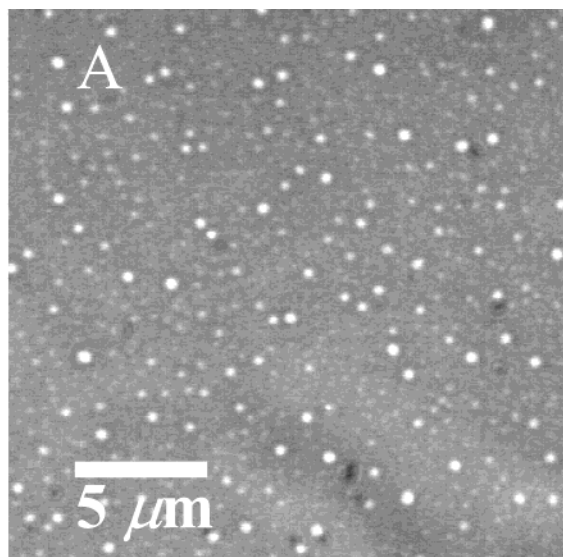


Figure 5. Phase contrast microscopy pictures of an inverted emulsion stabilized by POPC prepared by sonication. After several minutes, the suspension phase separates. Picture (A) shows the upper phase, which corresponds to the inverted emulsion that remains suspended in dodecane and picture (B) shows big emulsion drops, which have sedimented to the bottom of the sample vial and are full of vesicles.

equilibrated interface that is completely covered by lipids takes a surprisingly long time. This is most clearly demonstrated by the behavior of the surface tension of the oil–water interface in the presence of the lipids. Upon addition of the lipids, the surface tension of the interface decreases over several hours,²³ indicating the very slow equilibration time; by contrast, the surface tension of an oil–water interface stabilized by surfactants reaches equilibrium within seconds.²² This slow equilibration of the interface can affect the formation of both the inner and outer leaflets of the vesicle. To illustrate this, we studied the effect of adsorption on the formation of the inner monolayer using emulsions prepared by gentle stirring. We prepared an emulsion by stirring 0.5 vol % water into 20 mL of dodecane containing 0.05 mg/mL POPC with 1 mol % of NBD-PC. As the suspension was stirred, 0.5 mL of emulsion was collected after 60, 90, 120, and 180 min and placed over previously prepared intermediate/aqueous phases that had been allowed to equilibrate for 3 h, each consisting of 3 mL of the same stock

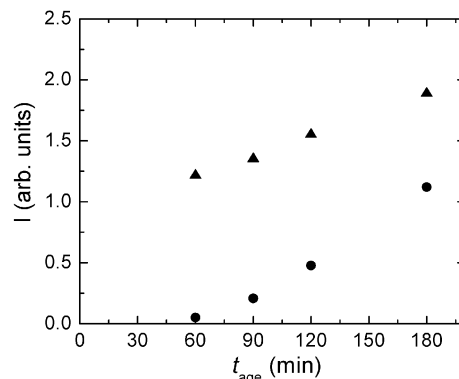


Figure 6. Increased fluorescence intensity for POPC vesicle suspensions produced with a fixed volume of emulsion removed after different amounts of stirring t_{age} . The increase in the fluorescence of the outer leaflet (triangles) indicates an increase in the number of vesicles produced, and the increase in the fluorescence of the inner leaflet (circles) indicates that NBD-PC enters the monolayer more slowly.

solution used for the emulsion placed over separate aqueous phases. These steps ensured that the interfaces between the aqueous and intermediate phase had reached equilibrium and that all these interfaces had the same composition.

The yield of vesicles produced from emulsions of different age was compared using fluorescence quenching techniques; results are shown in Figure 6. The fluorescence of both the outer (triangles) and the inner (circles) leaflets increases with the age of the emulsion used to make the vesicles. For the emulsion that had equilibrated the shortest time, the outer monolayer contributes 100% of the total fluorescence and the contribution due to the inner monolayer is negligible. For the most fully equilibrated emulsion, the contribution of the inner monolayer has increased to 40%. The outer leaflet is made from a fully equilibrated monolayer; the increase in fluorescence of this layer with equilibration time indicates that the efficiency of the vesicle production is increasing as the droplets equilibrate. The increase in fluorescence of the inner layer with equilibration time indicates that the tagged lipids, NBD-PC, adsorb at the interface of the emulsion droplets even more slowly than their undyed counterparts. These results suggest that a fully equilibrated interface should produce the best yield; however, we have prepared good quality vesicles with high yield in some instances where the interfaces were not fully saturated.

(3) *Controlling the Size of the Emulsion.* When surfactants are used to stabilize an inverted emulsion, the mean size of the droplets produced is set by the method of emulsification used and the amount and type of shear supplied to the suspension.²⁰ However, lipid-stabilized emulsions appear to behave significantly differently. This severely limits the possible control of the size of the emulsion drops and hence the size of the vesicles produced. To illustrate this problem, in this section we compare the distribution of sizes obtained for three inverted emulsions prepared at the same volume fraction but using three different techniques: sonication (for 5 min), high shear at 5000 rpm (5 min), and low shear (3 h). Experience with surfactant-stabilized emulsions suggests that the smallest drop size is expected for sonicated samples and the largest drop size is expected when the emulsion is formed by low-shear techniques.

We used DLS to measure the size of the inverted emulsions produced. In Figure 7A, we show the autocor-

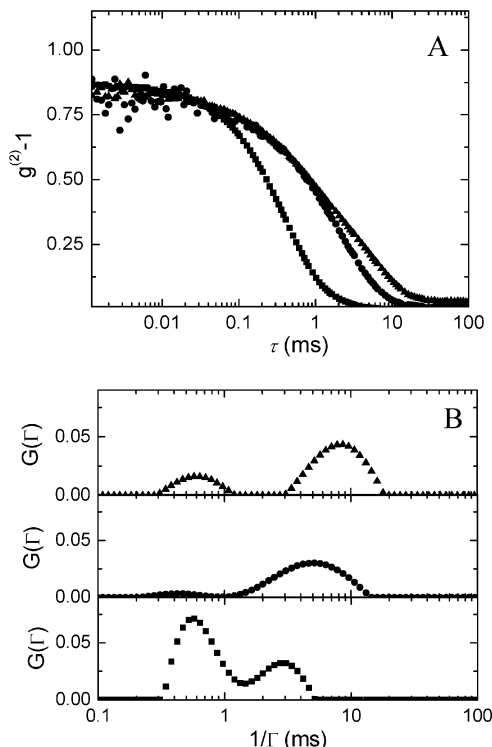


Figure 7. Dynamic light-scattering measurements at 90° for inverted emulsions stabilized by POPS and prepared using three different techniques; (A) $[g^{(2)}(\tau) - 1]$ for inverted emulsions prepared using sonication (squares), high-shear (circles), and low-shear (triangles) techniques. (B) Bimodal distribution of decay times. The first peak corresponds to a population of small droplets that has a similar size in all three samples and the second peak corresponds to a population of large droplets whose size depends on the emulsification technique.

relation functions measured for inverted emulsions stabilized with POPS and formed by sonication (squares), high shear (circles), or low shear (triangles). They are clearly not single exponential confirming that the emulsion is polydisperse. The distributions of decay rates are presented in Figure 7B. Two peaks corresponding to two distinct populations of droplets are observed in all three samples. There appears to be a population of large drops whose mean size varies with the amount of shear supplied to emulsify the suspension and a population of small drops with radii of about 150 nm that is present in each, independent of the emulsification method used. The fact that the small droplets occur independently of the method used suggests that these drops have been formed by some form of spontaneous emulsification²³ as has been observed in some surfactant systems.^{31,32} Thus, two emulsification processes are taking place: normal emulsification due to applied shear resulting in the larger drops and spontaneous emulsification leading to the smaller drops. When spontaneous emulsification occurs, it presents a serious limitation to our ability to control the size of the vesicles while preserving the concentration of vesicles. For example, it makes it difficult to efficiently produce large vesicles; to do so, a very low shear technique must be used to produce the emulsion, followed by further purification steps to isolate the larger droplets.^{21,33} Unfortunately, these purification steps compromise the efficiency of encapsulation, limiting the utility of this method.

(31) Rang, M.; Miller, C. A. *Progress in Colloid and Polymer Science*, Springer-Verlag: Berlin, 1998; Vol. 109.

(32) Rang, M.; Miller, C. A. *J. Colloid Interface Sci.* **1999**, *209*, 179.

(33) Kawashima, Y.; Hino, T.; Takeuchi, H.; Niwa, T.; Horibe, K. *J. Colloid Interface Sci.* **1991**, *145*, 512–523.

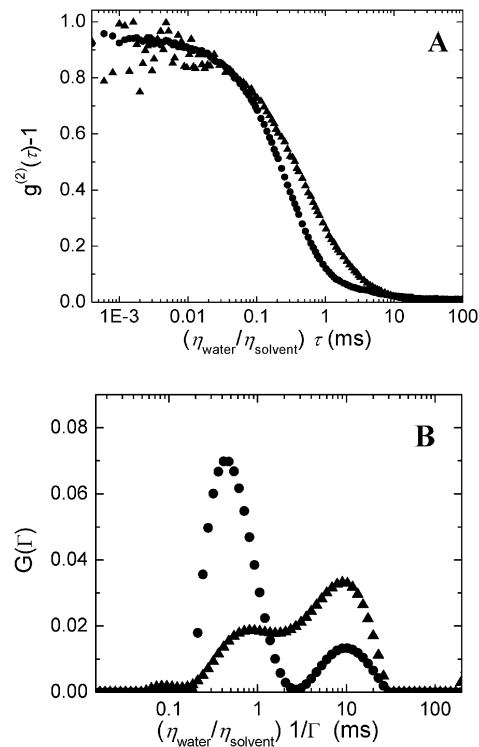


Figure 8. Comparison of the distribution of sizes between the emulsion and vesicles when the inverted emulsion contains large ($> 1 \mu\text{m}$) droplets. (A) DLS data taken at 90° for an inverted emulsion stabilized by POPS rescaled to take into account the difference in viscosity (triangles) and for the suspension of vesicles formed from this emulsion (circles). (B) Corresponding distribution of decay times for both samples. We observe differences between the distributions found for the emulsion (triangles) and that found for the vesicles (circles), particularly the loss of part of the largest inverted emulsion droplets upon sedimentation.

Alternatively, a direct scheme of droplet production^{33–35} may be used to restrict the formation of the emulsion drops to the desired size. For example, emulsions formed by extrusion can be used to produce large vesicles with relatively narrow size distributions, as we will show below.

(4) *Transfer of the Emulsion Droplets to the Aqueous Phase.* The outer monolayer is formed as the emulsion droplets pass through the interface between the intermediate and aqueous phases. Successful completion of this step depends on stability of the emulsion and coverage of the interface layer. As shown in Figure 3, we are able to obtain good transfer of small droplets, less than ~ 500 nm diameter.

Larger droplets present a much greater problem when they are transferred to the final aqueous phase. Figure 8 shows data for an inverted emulsion stabilized by POPS and prepared by gentle stirring and a solution of vesicles formed from it without fractionation. Figure 8A shows the autocorrelation function for the inverted emulsion (triangles) rescaled to take into account the difference in viscosity and the autocorrelation for the vesicles produced (circles). The two curves depart from each other at large correlation times indicating that larger drops are present in the emulsion. The corresponding decay time distributions are shown in Figure 8B; the two curves confirm that the population of large objects is much less important in

(34) Umbanhowar, P. B.; Prasad, V.; Weitz, D. A. *Langmuir* **2000**, *16*, 347–351.

(35) Thorsen, T.; Roberts, R.; Arnold, F.; Quake, S. *Phys. Rev. Lett.* **2001**, *86*, 4163–4166.

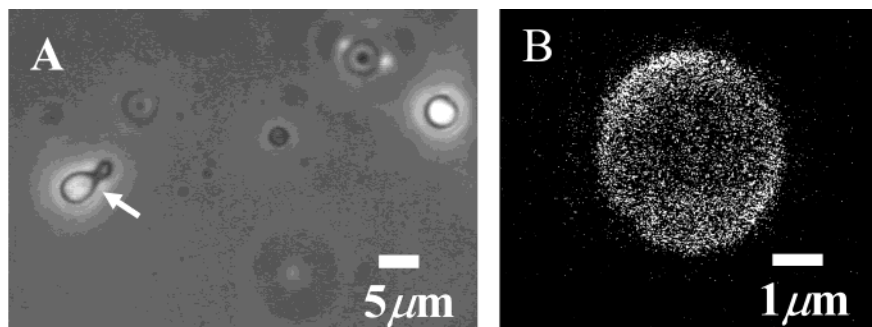


Figure 9. (A) Phase contrast microscopy image of Span80-egg-PC (80:20) vesicles. The arrow points to a budding vesicle. (B) Confocal microscopy image of a PABuPAM (diblock copolymer) vesicle tagged with 1 mol % NBD-PC. The distribution of the polarized fluorescence intensity confirms that the tagged lipids are incorporated into the polymer bilayer and are ordered normal to surface.

the vesicle solution than in the inverted emulsion. We believe that only a fraction of the large emulsion droplets pass through the interface to form vesicles because most break at the interface.

The breakage mechanism remains unclear, but experimental evidence suggests that the surface concentration of lipid at the oil–water interface plays an important role. This monolayer is also affected by the kinetics of interfacial lipid adsorption at the oil–water interface between the two bottom phases. We have observed in our study of asymmetric vesicles¹³ that several hours of equilibration time are also required to achieve sufficient lipid coverage of the intermediate phase monolayer for optimum conversion of emulsion droplets into vesicles, and that shorter equilibration times lead to an insufficient coverage and uncontrolled lipid composition. Unfortunately, when the interface is left to equilibrate for a much longer period of time, we observe a whitish cloud at the oil–water interface corresponding to an accumulation of lipid in multilayer structures. This very delicate balance between equilibration, which is required for the optimum formation of the vesicles, and spontaneous emulsification, which degrades the formation, creates a significant limitation in the technique. In practice, we allow this interface to equilibrate for more than two, but fewer than 3 h, providing the best compromise choice.

The depletion of lipid from the oil–water interface can also be responsible for transfer failure. As the emulsion droplets pass through the interface, they pick up part of the monolayer for bilayer completion. New lipids do not adsorb quickly enough to replenish the interface during the relatively fast sedimentation stage. This suggests that the area of the lower interface should be comparable to the total area of bilayer required for optimum vesicle production, which limits vesicle yield.

Applications

Here we present some applications that utilize this method of vesicle production; these examples exploit some of the advantages of this technique: the possibility of producing vesicles using a variety of bilayer constituents, the encapsulation efficiency, and the preservation of biological activity.

Polymer or Surfactant Constituent Molecules. This technique is not limited to lipids. Just as electroformation has been used to form more resistant polymeric vesicles from diblock copolymers,³⁶ this technique can be adapted for use with a wide variety of amphiphilic molecules to produce polymeric bilayers or mixed bilayers

where high encapsulation yield is preserved. In fact, a wide selection of amphiphilic molecules can be used as long as they can self-assemble at the oil–water interface and can stabilize an inverted emulsion. We have successfully made vesicles using inverted emulsions prepared with a wide variety of phospholipids both with and without added cholesterol, synthetic surfactants (either cationic or nonionic), and diblock copolymers. Two examples are presented in Figure 9.

In Figure 9A, we show a phase contrast microscopy image of vesicles prepared from an emulsion stabilized by 80:20 Span-80:egg-PC and formed by sonication. During the first 15 min following their formation, most of the largest vesicles presenting an excess area fluctuate and bud to form two smaller vesicles. The arrow shows a vesicle about to bud. Since we did not observe such behavior in other surfactants, we believe that the presence of Span-80 makes these vesicles more flexible leading to budding. After this reorganization, the vesicles remain stable for several days. When the percentage of Span-80 used is greater than 80%, the vesicles formed are unstable and break into micelles within a matter of hours.

An image obtained by confocal microscopy of one of the vesicles made with a diblock-copolymer PABuPAM, $M_w = 16\,000$ g/mol, tagged with 1 mol % NBD-PC is shown in Figure 9B. Nematic ordering of the molecules in the bilayer is observed in the polarization of the fluorescence; the brighter poles of the vesicle correspond to fluorescent light polarized parallel to the analyzer, and the darker poles correspond to fluorescent light polarized perpendicular to the analyzer, indicating that the fluorescent lipids are inserted in the polymer bilayer normal to the interface as in a lipid bilayer. Although this bipolarity is less pronounced than in a thinner lipid bilayer, it does suggest that the polymer bilayer is fairly ordered.

Microractors. Using this preparation technique, active molecules can be isolated from the bulk by encapsulating them in vesicles. Once encapsulated, macromolecules are unable to diffuse out, but a limited quantity of small molecules can diffuse from the bulk through the bilayer into the vesicles. Thus it is possible to design vesicles for use as microractors, where the reaction of macromolecules occurs in a controlled, isolated environment. This could have particular application in the encapsulation of biologically important molecules, provided their biological activity can be preserved during vesicle synthesis. To demonstrate the use of vesicles as microractors, it is necessary to show that the vesicles successfully encapsulate macromolecules, that we can control the transport of initiators across the bilayer, and that we can retain biological activity during the vesicle production process. As an example, we demonstrate the

(36) Discher, B. M.; Won, Y. Y.; Ege, D. S.; Lee, J. C. M.; Bates, F. S.; Discher, D. E.; Hammer, D. A. *Science* **1999**, *284*, 1143–1146.

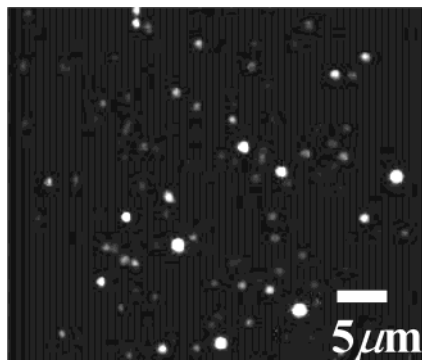


Figure 10. Vesicles formed from an emulsion stabilized by egg-PC:cholesterol (80:20), encapsulating $M_w = 10\,000$ dextran tagged with Texas Red, and produced by extrusion through a $2\text{-}\mu\text{m}$ -diameter filter. In this case, the vesicles are not bound to the substrate, so their intensity varies depending on their position in the focal plane.

polymerization of actin monomers triggered by an increase of the concentration of magnesium.

(1) *Encapsulation.* To demonstrate the encapsulation of macromolecules, we measured the fluorescence of $2\text{-}\mu\text{m}$ vesicles prepared from an egg-PC: cholesterol stabilized emulsion where the aqueous phase contained 1 wt % of a fluorescently labeled dextran ($M_w = 10\,000$ g/mol), a water-soluble polysaccharide. Using fluorescence microscopy, we observed that the fluorescence originates only in the interior of the vesicles with little background intensity, confirming that the dextran remains encapsulated within the vesicles, as shown in Figure 10. We have also been able to encapsulate dextran with $M_w = 200\,000$ g/mol.

(2) *Ion Transport across the Bilayer.* To demonstrate controlled ion transport, we encapsulated $10\,000$ M_w dextran conjugated with a calcium sensitive dye, Oregon Green, in vesicles with and without ionophores.³⁷ The ionophore used was A23187 (Sigma, St Louis); when present in the bilayer, it facilitates the transport of divalent cations across the bilayer. We used fluorescence spectroscopy to quantitatively measure changes in fluorescence intensity as a function of the concentration of calcium in the solution. As a control experiment, we first measured the fluorescence intensity ($\lambda_{\text{exc}} = 488$ nm, $\lambda_{\text{em}} = 535$ nm) of the conjugated dextran in bulk buffer solution before encapsulation as a function of the calcium added. Figure 11A shows the changes in the emission spectrum upon addition of calcium. The solid triangles correspond to the intensity of the emission spectrum for this dye without calcium in solution. After the addition of 5 mM calcium chloride, the intensity increased by a factor of 1.7, as shown by the open triangles.

The same polymer solution was then emulsified and encapsulated in vesicles. The vesicles were prepared with egg-PC:DOPS (80:20) with and without ionophores. In the presence of ionophores, calcium can diffuse into the vesicles until the concentration gradient is zero, with a corresponding increase in fluorescence intensity with time. Figure 11B shows the time dependence of the fluorescence intensity obtained for the encapsulated calcium-sensitive dextran. At time $t = 0$, we observe the fluorescence of the encapsulated polymer without calcium. The addition of 5 mM calcium to the vesicle suspension resulted in an increase of the fluorescence by a factor of 1.7, identical to that observed for the bulk sample. This confirms that the final concentration of calcium inside the vesicles is the

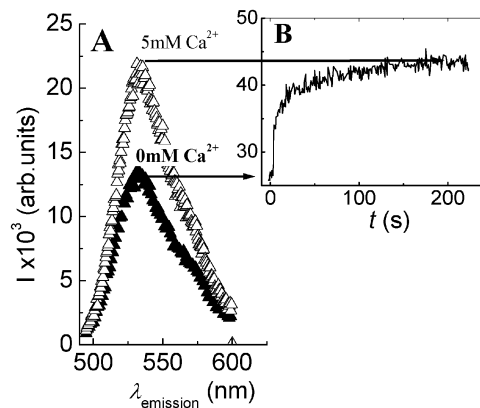


Figure 11. (A) Emission spectrum of dextran labeled with Oregon Green 488 bapta-1 at $\lambda_{\text{ex}} = 488$ nm. The solid triangles correspond to the emission spectrum of the dextran in buffer without calcium, and the open triangles show the changes in the emission spectrum after addition of 5 mM CaCl_2 in solution and are used to calibrate the fluorescent response for the addition of fixed amount of calcium. (B) Time course of the change in fluorescence intensity at $\lambda_{\text{em}} = 535$ nm for dextran encapsulated in egg-PC:DOPS vesicles upon addition of 5 mM CaCl_2 to the vesicle suspension. Ionophores have been incorporated into the bilayers to allow passive transport of divalent cations across the membrane. The curve shows how the fluorescence intensity changes as calcium ions diffuse into the vesicles.

same as the bulk concentration. In contrast, in a control experiment where vesicles were prepared without ionophores, we did not observe any detectable changes in fluorescence after addition of calcium to the suspension, confirming that ion transport across the membrane can be controlled using ionophores. Furthermore, this also quantitatively confirms our previous result that there is no measurable nonencapsulated dextran in the bulk solution and that dextran has been successfully encapsulated.

(3) *Biocompatibility.* A very important feature of vesicles is their biocompatibility. However, this emulsion-based production technique involves several transfers between fluids, not all of which may be completely compatible with biomaterials. To test the preservation of biological activity within our vesicles, we investigated the aggregation of G-actin to form F-actin. We encapsulated G-actin monomers from *acanthamoeba*¹⁴ in egg-PC vesicles with ionophores incorporated in the bilayer and studied the polymerization kinetics of the actin for two concentrations of encapsulated monomer: $5\ \mu\text{M}$ and $15\ \mu\text{M}$. To follow the kinetics of polymerization, we added 20% N-(1-pyrenyl)-iodoacetamide-labeled G-actin to the solution of actin monomer; the fluorescence of pyrene-labeled actin increases significantly upon polymerization, providing a sensitive probe of the reaction.¹⁵ We initiated the polymerization by the addition of salt to reach a final concentration of 50 mM KCl and 2 mM MgCl_2 .

The fluorescence intensity from both the encapsulated actin and a control sample of the same actin in bulk solution during the polymerization process for two actin concentrations is shown in Figure 12. A large difference in absolute intensities is measured between the bulk (symbols) and the encapsulated actin (curves), reflecting the dilution factor; the encapsulated data for both samples have been multiplied by a constant factor of 18.5 to rescale them to the same level as the bulk data.

Figure 12 shows that, in all cases, the addition of salt generates a strong increase in the fluorescent signal observed. The results obtained for $15\ \mu\text{M}$ actin in bulk

(37) Hackl, W.; Barmann, M.; Sackmann, E. *Phys. Rev. Lett.* **1998**, *80*, 1789.

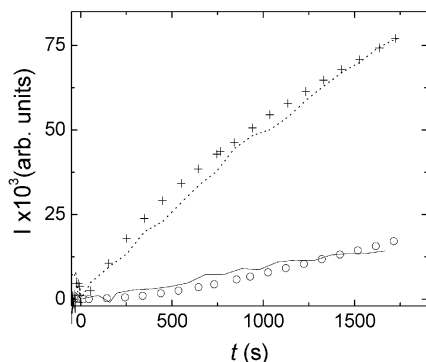


Figure 12. Fluorescence intensity of pyrene-labeled actin as a function of time after adding 50 mM KCl and 2 mM MgCl₂ to initiate polymerization. The symbols represent the kinetics of bulk actin at concentrations of 5 μ M (empty circles) and 15 μ M (plusses), while the curves are the kinetics of actin encapsulated in egg-PC vesicles at concentrations of 5 μ M (solid line) and 15 μ M (dotted line). The encapsulated actin data have been scaled by a constant consistent with the dilution factor.

(crosses) and the corresponding encapsulated actin (dotted line) overlap, confirming that the time dependence of the polymerization kinetics is identical. Similarly, the curve for 5 μ M actin in bulk (circles) overlaps with the corresponding encapsulated actin (solid line). These results confirm that the same polymerization reaction takes place within the vesicle as in bulk and that the concentration and protein activity are both preserved by the encapsulation technique.

The results also allow a measurement of encapsulation efficiency. The emulsion droplets that contain the actin have a total volume of 0.165 mL and are transferred into 3.0 mL of final aqueous phase. This results in a dilution factor of 18.2. Thus, for a 100% efficient process of encapsulation and transfer through the interface, the fluorescence of the vesicle suspension is expected to be 18.2 times smaller than the bulk sample. The measured scaling factor of 18.5 corresponds to 98% encapsulation efficiency.

Conclusions

The lipid behavior at oil–water interfaces makes it difficult to control the emulsification process and reduces the domain where this emulsion-based vesicle production technique produces optimal results. Some of these limitations can be mitigated by consideration of the phase behavior of the lipid/oil/water system and the kinetics of lipid adsorption. Once a protocol is designed that takes these limitations into account, the inverted emulsion

technique provides a way to simultaneously improve the encapsulation yield and to control the bilayer composition, while producing unilamellar lipid vesicles. We have shown that this technique can be used to prepare surfactant vesicles or polymersomes; in fact, the use of conventional surfactants or diblock copolymer improves our control of the emulsification process. We can encapsulate a wide variety of macromolecules at any desired concentration while preserving physiological conditions with encapsulation efficiencies of up to 98%. This technique is one of the very few means of conveniently encapsulating large macromolecules with radii of gyration as large as 1 μ m, as may be required for potential application such as drug delivery and gene therapy. Moreover, these carriers can be “functionalized” using biotin-conjugated lipids, providing a primary binding site for streptavidin. These vesicles can then react with the desired biotinylated antibodies and provide a convenient way to design immuno-liposomes,^{38–40} which can specifically bind to cellular receptors. Furthermore, we have demonstrated that this technique is compatible with biological activity and that the vesicles produced with this method can be used as micro-bioreactors. This provides the possibility of controlling reactions in a confined space. This method also offers a new way to design chemical sensors where vesicles could be used to locally probe the ion concentration in solution as well as multiencapsulation devices with vesicles containing sub-compartments filled with different molecules. In summary, emulsion-based vesicle production provides a new means of making vesicles that may find uses in a wide range of materials science.

Acknowledgment. We thank E.M. Ostap for assistance in purifying G-actin and for use of his laboratory for the actin experiments and G. Whitesides for use of his spectrofluorimeter. We are grateful to J. Crocker, D. Discher, and E. Weeks for their useful suggestions. S.P. is particularly grateful to C. Gay and M.T. Valentine for help in the preparation of this article and to P. Poulin for his encouragement at the early stage of this work and for discussions as the project progressed. We also thank Rhodia (Cranbury, NJ) for supplying the diblock copolymers. This work was supported by Rhodia, Kraft Foods, and by the NSF (DMR-9971432).

LA026100V

(38) Szebeni, J. *Crit. Rev. Therapeutic Drug Carrier Systems* **1998**, *15*, 57–88.

(39) Park, J. W.; Hong, K.; Kirpotin, D. B.; Papahadjopoulos, D.; Benz, C. C. *Immunoliposomes for Cancer Treatment*; Academic Press: New York, 1997; Vol. 40.

(40) Harokopakis, E.; Hajishengallis, G.; Michalek, S. M. *Infect. Immun.* **1998**, *66*, 4299–4304.